Available online at www.sciencedirect.com
SCIENCE DIRECT
Physics Letters A 356 (2006) 255–261
PHYSICS LETTERS A
www.elsevier.com/locate/pla

Photoinduced indirect transitions and ultrafast direct current generation in unbiased superlattices

A.S. Moskalenko *,[1], A. Matos-Abiague, J. Berakdar

Max-Planck-Institut für Mikrostrukturphysik, Weinberg 2, 06120 Halle, Germany

Received 27 December 2005; received in revised form 14 February 2006; accepted 24 March 2006

Available online 3 April 2006

Communicated by B. Fricke

Abstract

We theoretically analyze the electron dynamics in a superlattice (SL) driven by a highly asymmetric electromagnetic pulse. We show that the time asymmetry of the pulse results in indirect population of higher minibands and leads to the appearance of a direct current. At low temperatures and low filling of the lowest miniband the current generated in the SL has an oscillating behavior as a function of the pulse strength with minima occurring when the wave vector transferred by the pulse matches an integer of half the reciprocal lattice constant.

PACS: 72.20.Ht; 73.21.Cd; 42.65.Re

Keywords: Superlattices; Half-cycle pulses; Ultrafast; Photocurrent

1. Introduction

Considerable efforts in condensed matter research are devoted to the study of semiconductor superlattices (SLs) due to their importance for quantum cascade lasers [1,2] and to their fundamental significance for fabricating materials with desirable band-structure properties [3,4].

Recently, the novel phenomena of the quantum ratchet effect [5–7] and the rectification of alternating fields due to wave mixing [8,9] in unbiased periodic systems have been investigated. A paradigm of a quantum ratchet is the motion of a quantum Brownian particle in an asymmetric, periodic *ratchet* potential in the presence of quantum Brownian fluctuations. If the ratchet potential is tilted alternately by an unbiased adiabatic switching, quantum mechanics (in contrast to the classical expectation) predicts the existence of a finite direct current (DC) [5–7]. For the appearance of such a DC, the asymmetry of the periodic potential and the presence of a quantum noise are crucial. Other schemes for rectifying unbiased alternating fields in SLs in the nonadiabatic regime have also been proposed [8–11]. In particular, it has been shown that the use of a wave mixing of an alternating electric field and its second harmonic in a single miniband of an unbiased SL can lead to the generation of a DC which is a result of dissipation effects [8,9] and/or of the nonparabolicity of the electron energy bands [9].

In the present Letter we theoretically analyze the effect of direct current generation in unbiased semiconductor SLs upon irradiation by so-called half-cycle pulses (HCPs). HCPs are nearly unipolar electromagnetic pulses whose electric field resembles one-half of an optical oscillation cycle with duration τ_d followed by a much longer decaying tail of duration τ_t, opposite polarity, and of much smaller amplitude (for details on the experimentally realized HCPs see Refs. [12–15]). In contrast to the previously proposed procedures, the current generation effect investigated here does not rely on dissipation nor nonparabolicity effects but on the highly asymmetric nature of such pulses. It has been shown that in the far field the time integral of the electric field over the whole duration of the HCP vanishes but in the near field the integral over the positive part of

* Corresponding author. Tel.: +49 345 5582909; fax: +49 345 5582765.
E-mail address: moskalen@mpi-halle.de (A.S. Moskalenko).
[1] Also at A.F. Ioffe Physico-Technical Institute, 194021 St. Petersburg, Russia.

0375-9601/$ – see front matter
doi:10.1016/j.physleta.2006.03.061

the pulse can be much larger than the integral over the long negative tail [14,15]. Here we consider this specific case of the HCP shape and the ballistic regime, when τ_d is much shorter than the carrier relaxation time. If, in addition, $\tau_d < \tau_{\rm sys}$, where $\tau_{\rm sys}$ denotes the shortest time scale characterizing the dynamics of charge carriers (a more detailed explanation of this quantity for the case of charge carriers in a SL is given in Section 3), the HCP imparts a net (directed) wave vector change to the electronic system. This peculiarity of the matter-HCP interaction is the foundation of a variety of phenomena occurring in HCP-driven atoms [13,16], molecules [17,18] and mesoscopic heterostructures [19,20] that cannot be achieved by utilizing multicycle pulses. In the present case of HCP-driven SLs we expect the pulse to deliver to the carriers in the SL a definite amount of unidirectional wave vector that is determined by the time-integral over the pulse electric field whilst the HCP polarity governs the direction of the wave-vector transfer. This type of interaction yields excited states with a broken time-reversal symmetry and hence a finite DC emerges. This anticipation is quantified below and the magnitude of the generated current is calculated numerically. One should mention that other aspects of the interaction of ultrashort monopolar electromagnetic pulses with thin SL layers were theoretically studied in the past and several nonlinear effects concerning transmission properties were predicted [21–23].

The Letter is organized as follows. In Section 2 we present a simplified model for the SL and calculate the overlaps between the eigenstates of the SL. These overlaps are then used in Sections 3 and 4 for obtaining the population changes in the minibands and the current induced by the HCP, respectively. The total current consists of a DC part, which is constant in time (neglecting relaxation), and an oscillating interminiband part. For the case of a low filling of the lowest miniband the dependence of the DC on the strength of the HCP has minima when the wave vector p transferred by the pulse equals an integer of half the reciprocal lattice constant. In the event that the lowest miniband is completely filled, higher minibands should be populated for creating a net current and, therefore, there is a finite critical value of p below which the induced DC is almost zero. Conclusions are made in Section 5.

2. Energy spectrum and eigenfunctions of the model superlattice

We consider a one-dimensional SL with a spatial period a. According to the Bloch theorem the corresponding eigenfunctions are expressible in the following form

$$\psi_q(x) = \frac{1}{\sqrt{L}} u_q(x) \mathrm{e}^{iqx}, \tag{1}$$

where $u_q(x)$ are the Bloch amplitudes, which are spatially periodic functions with period a. The wave vector q varies within the range $-\pi/a < q < \pi/a$. Denoting by N the total number of unit cells, the length of the SL is determined by $L = aN$.

The overall physical conclusions and results discussed in this Letter do not depend on the particular shape of the potential barriers defining the SL. For the sake of simplicity and clarity we assume here that the SL is formed by a periodic distribution of potential barriers having the shape of Dirac delta functions (see Fig. 1), separated by a distance a from each other. By appropriately adjusting the strength of the delta peaks, as done below, the band structure of such a model system reflects well the band structure of real semiconductor SLs.

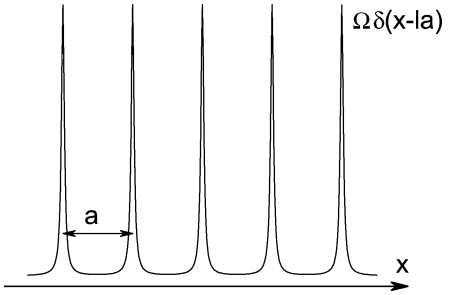

Fig. 1. Periodic potential consisting of Dirac delta functions (Dirac comb). The period of the SL is denoted by a and Ω represents the strength of a single peak.

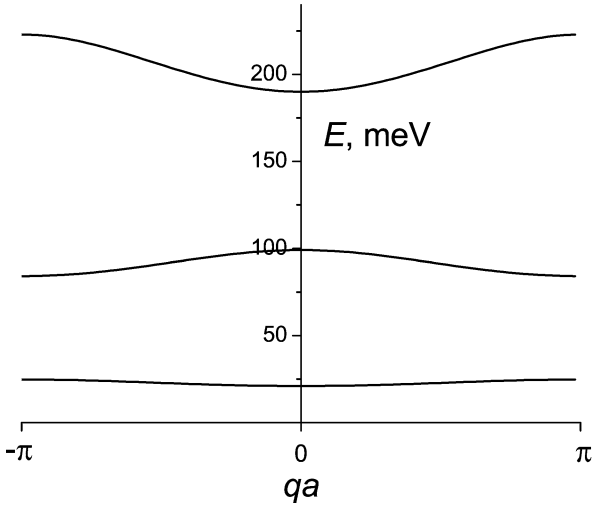

Fig. 2. Energy miniband structure for the parameters: $a = 15$ nm, $m = 0.067m_0$, $\Omega = 23\hbar^2/(ma)$. The strength of the barrier Ω is chosen as to ensure a good agreement for the energy width of the first miniband and the gap between the second and the first minibands calculated within the Kronig–Penney model [26].

The energy spectrum $E = \hbar^2 k^2/(2m)$ (here m is the electron effective mass) of the SL is given by the well-known relation [24,25]

$$\cos(ka) + \frac{m\Omega}{k\hbar^2}\sin(ka) = \cos(qa), \tag{2}$$

which for each value of q has solutions $k_n(q)$ belonging to the different minibands which are labeled here with the index n. The structure of the three lowest minibands of our SL is shown in Fig. 2 for a case in which a good agreement with the respective minibands of an $Al_{0.32}Ga_{0.68}As/GaAs$ SL is achieved.

The Bloch amplitudes in the range $x \in [0, a]$ can be written in the following form [25]

$$u_{n,q}(x) = A_{n,q}\left[\left(\mathrm{e}^{iqa} - \mathrm{e}^{-ika}\right)\mathrm{e}^{ikx} + \left(\mathrm{e}^{ika} - \mathrm{e}^{iqa}\right)\mathrm{e}^{-ikx}\right] \times \mathrm{e}^{-iqx}, \tag{3}$$

where the normalization coefficients

$$A_{n,q} = \frac{1}{2}\Big\{\big[1-\cos(ka)\cos(qa)\big] + \frac{\sin(ka)}{ka}\big[\cos(qa)-\cos(ka)\big]\Big\}^{-1/2} \tag{4}$$

are such that the integral over the unit cell of $|u_{n,q}(x)|^2$ equals a. For the case $x \notin [0,a]$, the Bloch amplitudes are found from Eq. (3) by making use of the translation invariance symmetry, i.e., $u_{n,q}(x+la) = u_{n,q}(x)$, with l being an integer number. Here and in what follows we write k instead of $k_n(q)$, for simplicity of notations.

The overlaps between two different Bloch amplitudes are defined as

$$T^{n,q}_{n',q'} = \frac{1}{a}\int_0^a \mathrm{d}x\, u^*_{n',q'}(x)u_{n,q}(x). \tag{5}$$

From Eqs. (3) and (5) one obtains

$$\begin{aligned} T^{n,q}_{n',q'} = {} & \frac{4}{a}A_{n,q}A_{n',q'} \\ & \times\Bigg\{\frac{(k-k')\sin[(k-k')a]}{(k-k')^2-(q-q')^2} - \frac{(k+k')\sin[(k+k')a]}{(k+k')^2-(q-q')^2} \\ & - \frac{k'\sin[(k+q')a]}{(k-q+q')^2-k'^2} - \frac{k'\sin[(k-q')a]}{(k+q-q')^2-k'^2} \\ & + \frac{k\sin[(q+k')a]}{k^2-(q+k'-q')^2} - \frac{k\sin[(q-k')a]}{k^2-(q-k'-q')^2} \\ & - \frac{(q-q')\sin[(q-q')a]}{(k-k')^2-(q-q')^2} + \frac{(q-q')\sin[(q-q')a]}{(k+k')^2-(q-q')^2}\Bigg\}. \end{aligned} \tag{6}$$

Here and in what follows $k_{n'}(q')$ is written simply as k'.

3. Electron excitations in a SL driven by a HCP

A key feature of a HCP that makes its action on an electron system different from the action of multicycle symmetric pulses, is mostly pronounced when the duration of the HCP is much shorter than the characteristic times τ_{sys} of the electron system. In such a case the so-called impulsive approximation (IA) [27,28] applies and the action of the HCP on an electron can be described as the transfer of a wave vector $p = \frac{e}{\hbar}\int_{-\infty}^{\tau_d} E(t)\,\mathrm{d}t$, where $E(t)$ is the electric field of the HCP, e is the electron charge and τ_d is the duration of the HCP. We stress that because of the asymmetric nature of the HCP, p acquires, in the near field, a finite value (even when the upper integration limit is extended to infinity) [15]. For example if we assume, as done here, that the pulse shape is given by $E(t) = E_0\sin^2(\pi t/\tau_d)$ for $0 < t < \tau_d$ and $E(t) = 0$ otherwise then $p = eE_0\tau_d/(2\hbar)$.

Accessing the impulsive regime in a SL requires $\tau_d < \tau_{\mathrm{sys}}$ where $\tau_{\mathrm{sys}} = \hbar/\max\{E_{q_f,n_f} - E_{q_i,n_i}\}$ is determined by the transition from the lowest occupied initial electron state with energy E_{q_i,n_i} to the highest excited final state with energy E_{q_f,n_f}. As shown below, the stronger the HCP the higher the minibands that are excited. Therefore, generally the applicability of the IA depends not only on the duration of the pulse but also on the pulse strength. For the miniband structure displayed in Fig. 2 one obtains for excitations involving interband transitions between neighboring bands $\tau_{\mathrm{sys}} \approx 8$ fs and for transitions from the first to the third miniband $\tau_{\mathrm{sys}} \approx 3$ fs. Thus, femtosecond HCPs are generally required for accessing the impulsive regime when interband transitions are involved. We remark, that currently available HCPs [12,13] are much longer than those required here. However, the realization of HCPs with duration even shorter than 1 femtosecond is already discussed in the literature [29]. Another way to overcome this limitation is to use SLs with larger spatial periods. Furthermore, for excitations involving intraband transitions only, τ_{sys} can be in the desired range.

Within the IA, the single-particle wave functions just before ($t = 0^-$) and right after ($t = 0^+$) the application of the HCP are related through the following matching condition [27]

$$\Psi\big(x, t = 0^+\big) = \Psi\big(x, t = 0^-\big)\mathrm{e}^{ipx}, \tag{7}$$

where p is the wave vector transferred by the pulse. The time-dependent wave function $\Psi_{n,q}(x,t)$ corresponding to a particle being initially (i.e., before the application of the HCP) in the nth band with wave vector q can be written as follows

$$\Psi_{n,q}(x,t) = \sum_{n',q'} C^{n,q}_{n',q'}(t)\mathrm{e}^{-\frac{i}{\hbar}E_{n',q'}t}\psi_{n',q'}(x). \tag{8}$$

We note that the sum over q' corresponds to the case of a finite SL and can be approximated by an integral if the SL contains a large number N of unit cells.

From Eqs. (1), (7), and (8), we obtain

$$C^{n,q}_{n',q'}(t) = \delta_{n,n'}\delta_{q,q'}, \quad \text{for } t < 0, \tag{9}$$

$$C^{n,q}_{n',q'}(t) = \sum_{G_j}\delta_{q',q+p+G_j}\frac{1}{a}\int_0^a \mathrm{d}x\, u^*_{n',q'}(x)u_{n,q}(x)\mathrm{e}^{-iG_jx}, \quad \text{for } t > 0. \tag{10}$$

The sum over all the possible reciprocal lattice vectors $G_j = j\frac{2\pi}{a}$ ($j \in \mathbb{Z}$) is restricted by the condition that $q' = q + p + G_j$ belongs to the first Brillouin zone (BZ). Comparing Eq. (10) with Eq. (5) we can write

$$C^{n,q}_{n',q'}(t) = T^{n,q}_{n',q+p}, \quad \text{for } t > 0. \tag{11}$$

Eq. (6) is then used for these coefficients, where the wave vector $q + p$ can also be now outside the first BZ (notice that Eqs. (1) and (4) do not change by shifting the wave vector q by a reciprocal lattice vector G_j).

The magnitudes $|C^{n,q}_{n',q'}(t)|^2$ of the transition coefficients yield the probabilities for an electron being initially in the nth miniband with wave vector q to be detected in the n'th miniband with the wave vector q' after application of the HCP. In Figs. 3(a), (b), and (c) we show the probability of an electron from the lowest (first) miniband with wave vector q to be found in the first, second and third minibands, respectively, after application of a HCP. The strength of the pulse is such

that it transfers a wave vector p to the electron (recall that the wave vector q' of the excited state is fixed by the constraint that $q' = q + p + G_j$ should be in the first BZ). Note that, in contrast to conventional direct optical transitions induced by continuous wave lasers and standard laser pulses, HCPs induce indirect transitions between different minibands of a SL which involves a large wave-vector transfer, as evident from Fig. 3. Notice that for a semiconductor SL with $a = 15$ nm in order to reach $pa = \pi$ the peak electrical field of a HCP with 1 fs duration should be on the order of 1 MV/cm. For a semiconductor SL with a spatial period of $a = 150$ nm and a HCP with 100 fs duration the peak electrical field should be on the order of 1 kV/cm.

One can also see from Fig. 3 that upon application of the HCP the reflection symmetry with respect to the center $q = 0$ of the first BZ breaks down. Consequently, an asymmetric population with respect to $q' = 0$ will also develop (this is particularly clear when $pa = 2n\pi$ ($n \in \mathbb{Z}$), for in this case the constraint that $q' = q + p + G_j$ must belong to the first BZ leads to $q' = q$), suggesting that a finite current could be generated by the pulse in dependence of the initial population of the minibands. Furthermore, opposite polarities (p and $-p$) of the pulse lead to the same populations on the opposite sides of the first BZ, i.e., by reversing the polarity of the pulse the direction of the induced current must also be reversed. Note, however, that the reverse of the pulse polarity should leave invariant the absolute value of the current, since we assumed a SL with inversion symmetry. This fact is reflected in the invariance of Figs. 3(a), (b), and (c) under the transformation ($p \to -p, q \to -q$).

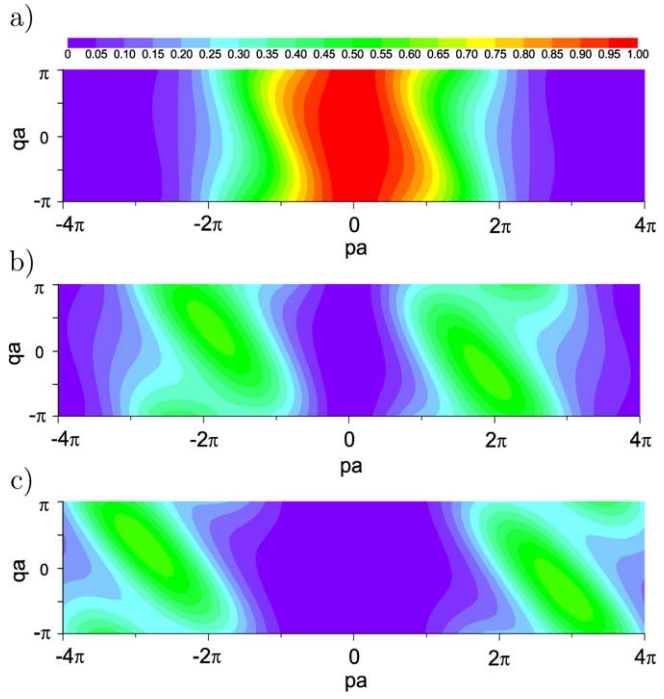

Fig. 3. Probability right after the application of a HCP for an electron to be in: (a) first, (b) second, (c) third miniband. Initially the particle resides in the first miniband and has wave vector q. The probability is shown as a function of qa and the scaled pulse strength pa. The same value of Ω as in Fig. 2 was used.

4. Current generation

In this section we investigate in detail the characteristics and properties of the current created by a HCP in a SL.

The charge current $i_{n,q}(t)$ carried by a particle that is described by the wave function $\Psi_{n,q}(x,t)$ (see Eqs. (8)–(10)) is determined by

$$i_{n,q}(t) = \frac{1}{L}\int_{-L/2}^{L/2} \mathrm{d}x\, \frac{ie\hbar}{2m}\left(\Psi_{n,q}(x,t)\frac{\mathrm{d}}{\mathrm{d}x}\Psi^*_{n,q}(x,t) - \Psi^*_{n,q}(x,t)\frac{\mathrm{d}}{\mathrm{d}x}\Psi_{n,q}(x,t)\right). \tag{12}$$

One can change the integration over the SL length L to an integration over the unit cell in Eq. (12) and perform a summation over all cells by using the periodicity of the Bloch amplitudes. Then, taking into account that before application of the HCP the particles are in stationary states given by Eqs. (1)–(4), one obtains the following expression for the current carried by a particle with wave vector q in the nth miniband before the pulse application,

$$i^{(0)}_{n,q} = \frac{1}{L}\frac{e\hbar q}{m^{\mathrm{eff}}_n(q)}, \tag{13}$$

where we have introduced the effective mass

$$m^{\mathrm{eff}}_n(q) = m\frac{q}{4kA^2_{n,q}\sin(ka)\sin(qa)}. \tag{14}$$

The dependence of the effective mass on the wave vector q is displayed in Fig. 4 for the three lowest minibands. For the center of the BZ ($q = 0$) the value of the effective mass given by Eq. (14) coincides with the value calculated by the definition

$$m^{\mathrm{eff}}_n(q) = \left(\frac{\partial^2 E_n(q)}{\partial q^2}\right)^{-1}. \tag{15}$$

It is worth noting that Eq. (13) can also be obtained by using $i^{(0)}_{n,q} = ev^{(0)}_{n,q}/L$, where $v^{(0)}_{n,q} = \hbar^{-1}\partial_q E_n(q)$ is the velocity and $E_n(q)$ is the energy of the particle.

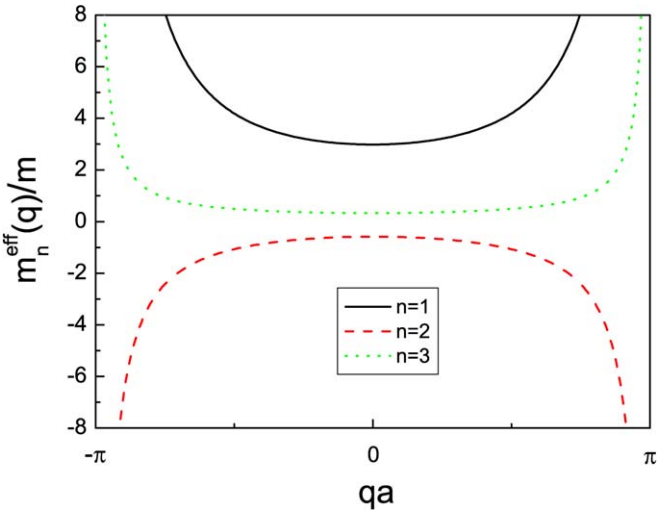

Fig. 4. Dependence of the effective mass on the wave vector q for the three lowest minibands. The same parameters as in Fig. 2 were used.

One can also find from Eqs. (1), (7), and (12) that the corresponding single particle current right after the pulse application ($t = 0^+$) is determined by

$$i_{n,q}\big(t=0^+\big) = i^{(0)}_{n,q} + \frac{e\hbar p}{mL}, \tag{16}$$

i.e., each electron in the SL has gained an additional momentum $\hbar p$ from the HCP. On the other hand, neglecting relaxation effects, and using Eqs. (8), (11), and (12) we get for $t > 0$ the following relation

$$\begin{aligned} i_{n,q}(t>0) = {} & \sum_{n'} \big|T^{n,q}_{n',q+p}\big|^2 j_{n',n'}(q+p) \\ & + \sum_{n',n''(n'\neq n'')} T^{n,q}_{n',q+p} T^{n,q}_{n'',q+p} j_{n',n''}(q+p) \\ & \times \cos\left[\frac{(E_{n',q+p} - E_{n'',q+p})t}{\hbar}\right], \end{aligned} \tag{17}$$

where

$$\begin{aligned} j_{n,n'}(q) = {} & \frac{8e\hbar}{Lma} A_{n,q} A_{n',q} \frac{kk'}{k^2 - k'^2} \sin(qa) \\ & \times \big(\cos(k'a) - \cos(ka)\big). \end{aligned} \tag{18}$$

The first sum in the right-hand side of Eq. (17) corresponds to stationary-like contributions (note by comparing Eqs. (13) and (18) that $j_{n,n}(q) = i^{(0)}_{n,q}$) while the second sum accounts for interference effects.

The total current, created by the carriers having in the initial state distribution function $f_{n,q}(\mu, T)$ (here $f_{n,q}(\mu, T)$ is the Fermi–Dirac distribution function multiplied by two to account for the twofold spin degeneracy), where $\mu = \mu(N)$ is the chemical potential determined by the number of electrons N and T is the temperature, is given by

$$I(t) = \sum_{n,q} f_{n,q}(\mu, T) i_{n,q}(t). \tag{19}$$

The substitution of Eqs. (13) and (14) into (19) gives a zero value for the net current before the pulse application. Making use of Eqs. (16) and (19) one obtains, however, that the net current right after the application of the HCP acquires the finite value

$$I\big(t=0^+\big) = \frac{e\hbar p}{m} n_{1D}, \tag{20}$$

where

$$n_{1D} = \frac{1}{L} \sum_{n,q} f_{n,q}(\mu, T) \tag{21}$$

denotes the one-dimensional electron density. Furthermore, one obtains from Eqs. (17) and (19) that the total current for $t > 0$ is given by

$$I(t>0) = I_{DC} + I_{AC}(t), \tag{22}$$

where the DC part of the total current is the sum of intraminiband $[i^{\text{intra}}(p)]$ and interminiband $[i^{\text{inter}}(p)]$ current contributions, i.e.,

$$I_{DC} = i^{\text{intra}}(p) + i^{\text{inter}}(p) \tag{23}$$

with

$$i^{\text{intra}}(p) = \sum_{n,q} f_{n,q}(\mu, T) \big|T^{n,q}_{n,q+p}\big|^2 i^{(0)}_{n,q+p}, \tag{24}$$

$$i^{\text{inter}}(p) = \sum_{n,n',q(n\neq n')} f_{n,q}(\mu, T) \big|T^{n,q}_{n',q+p}\big|^2 i^{(0)}_{n',q+p}. \tag{25}$$

On the other hand, the AC part of the total current can be written as

$$\begin{aligned} I_{AC}(t) = {} & \sum_{n,n',n'',q(n'\neq n'')} f_{n,q}(\mu, T) T^{n,q}_{n',q+p} T^{n,q}_{n'',q+p} j_{n',n''}(q+p) \\ & \times \cos\left[\frac{(E_{n',q+p} - E_{n'',q+p})t}{\hbar}\right]. \end{aligned} \tag{26}$$

The above expression demonstrates that the AC component of the total current arises, exclusively, from interference effects involving interminiband transitions.

It is not difficult to prove that Eqs. (16) and (22) give the same result for $t = 0^+$. For subsequent time moments the AC contribution $I_{AC}(t)$ to the total current oscillates in time having zero average value. Consequently, the net charge transfer is caused only by the constant DC contribution I_{DC}.

In Fig. 5 we show the dependence of the current generated right after the pulse $I(t = 0^+)$ on the transferred wave vector p for different values of the initial filling n_{1D} of the lowest miniband. The thin dotted line represents the exact (within the IA) result computed using Eq. (20). The other lines correspond to an approximation neglecting excitations beyond the four lowest minibands. As one can clearly see, for the shown range of the transferred wave vector p the result of the four-minibands approximation is in good accord with the linear behavior of the

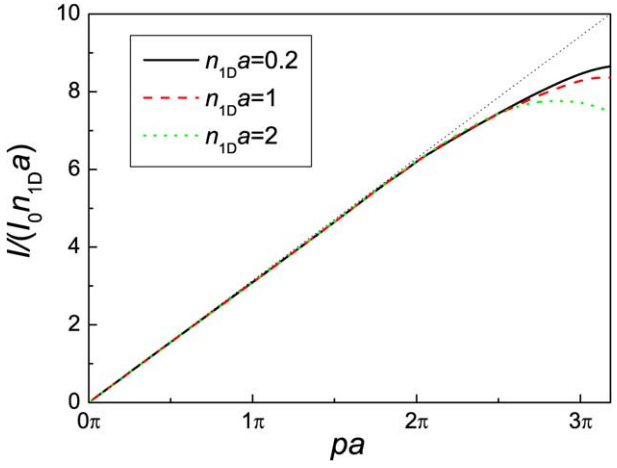

Fig. 5. Current $I(t = 0^+)$ (in units of $I_0 n_{1D} a$, where I_0 is defined by Eq. (27)) generated right after the pulse excitation as a function of the wave vector transferred by the HCP. The thin dotted line shows the linear dependence given by Eq. (20). All other lines show results of approximative calculations using Eqs. (22)–(26), and accounting only for the four lowest minibands. Full line shows the case of the low initial filling of the first miniband with $n_{1D}a = 0.2$, dashed line shows the case of the half-filled first miniband with $n_{1D}a = 1$, and the dotted line corresponds to the filled first miniband with $n_{1D}a = 2$. The strength of the delta-peaks of the superlattice is $\Omega = 23\hbar^2/(ma)$. Temperature $T = 0$.

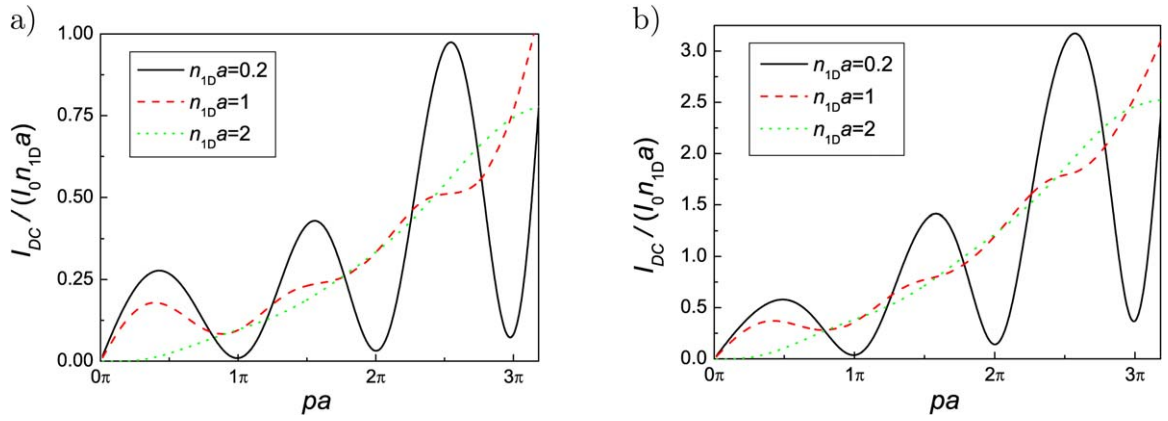

Fig. 6. Dependence of the normalized direct current $\tilde{I} = I_{\mathrm{DC}}/(I_0 n_{1\mathrm{D}} a)$ on the normalized transferred wave vector pa. The strength of the delta peaks of the SL is: (a) $\Omega = 23\hbar^2/(ma)$, (b) $\Omega = 10\hbar^2/(ma)$. Full, dashed, and dotted lines correspond, respectively, to low filling ($n_{1\mathrm{D}}a = 0.2$), half-filling ($n_{1\mathrm{D}}a = 1$), and complete filling ($n_{1\mathrm{D}}a = 2$) of the first miniband at zero temperature.

exact result. Consequently, within the range of parameters assumed here, it is enough to consider transitions between the four lowest minibands to accurately describe the system. This justifies the validity of the four-minibands approximation used for obtaining all the results presented below.

In order to investigate the dependence of the DC on the strength of the HCP, which is characterized by the transferred wave vector p, we consider the case of $T = 0$ and suppose that initially (i.e., before application of the pulse) only the first miniband is populated. In Fig. 6 we show the dependence of the normalized DC $\tilde{I} = I_{\mathrm{DC}}/(I_0 n_{1\mathrm{D}} a)$ on the normalized transferred wave vector pa. Here

$$I_0 = \frac{e\hbar}{ma^2}, \tag{27}$$

and $n_{1\mathrm{D}}a$ is the factor characterizing the filling of the first miniband ($n_{1\mathrm{D}}a = 2$ for the first miniband being completely filled; the factor 2 appears here because of two-fold spin degeneracy). For a SL with $a = 15$ nm and $m = 0.067m_0$ we have $I_0 \approx 1.2$ μA. Remember that here for the sake of simplicity we consider strictly one-dimensional SLs. The DC in a SL having spatial extension in the plane perpendicular to the axis of the SL (x-axis in Fig. 1) is the larger the large is this extension. By calculating the dependence of the DC on the transferred wave vector we took into account all transitions of the four lowest minibands. In Fig. 6(a) we used $\Omega = 23\hbar^2/(ma)$ that corresponds to the energy band structure of Fig. 2. For comparison in Fig. 6(b) we show the same dependence but for a lower effective energy barrier height $\Omega = 10\hbar^2/(ma)$. The dependence is similar but the current has larger values. Generally, in the case of high energy barriers, which is close to the situation of single atoms, the DC is low, and in the case of small energy barriers, which is close to the situation of free electrons, the DC converges to the current created just after the pulse (see Eq. (20)).

From the constraint that $q' = q + p + G_j$ must belong to the first BZ (see Section 3) we conclude that $q' = q$ if $p = 2n\pi/a$ ($n \in \mathbb{Z}$) and $q' = q - \mathrm{sgn}(q)\pi/a$ if $p = (2n+1)\pi/a$. Therefore, for an initially small population of the lowest miniband (i.e., if all the carriers have small q-values before the pulse application) a HCP with $pa = 2n\pi$ transfers the electrons to the vicinity of the center of the BZ and the initial reflection symmetry (with respect to $q = 0$) of the minibands population is approximately recovered after the application of the pulse. On the other hand if $pa = (2n + 1)\pi$ the electrons are transferred to the vicinity of the boundaries of the BZ, where the effective mass rapidly increases (see Fig. 4). Consequently, the induced DC exhibits minima at $pa = n\pi$ ($n \in \mathbb{Z}$), as evidenced by Fig. 6. Furthermore, when the transferred wave vector pa increases higher minibands become involved and the reflection asymmetry behaves as discussed and illustrated by Figs. 3(a), (b), and (c). Hence, the values of the minima of the induced DC increase as the integer values of pa/π increase (see Fig. 6).

In contrast to the situation discussed above, when the filling of the lowest miniband is increased the transfer of electrons at integer values of pa/π is no longer limited to the central and boundary regions of the BZ but involves transitions, in general, along the entire BZ (this is particularly true in the case when the lowest miniband is completely filled). These processes involving initial q values along the entire BZ lead to an appreciable enhancement of the population asymmetry of the minibands (see Fig. 3). As a consequence, the minima of the induced DC at integer values of pa/π are progressively smoothed out when increasing the lowest miniband population and completely disappear in the case of a full miniband. This behavior is quite apparent in Fig. 6. One can also appreciate that if the miniband is initially filled then there is a critical value p_c for the transferred wave vector needed to generate a current (see dotted lines in Fig. 6). Below this critical value the current also increases when the transferred wave vector increases but much slower than above p_c. This is due to the fact that in such a case in order to create a current electrons should be transferred into the second or higher minibands. The existence of a range of transferred wave vectors around zero for which no excitations of the second or higher bands take place (see Fig. 3) results then in a finite value of p_c.

We note that although interband excitations are not generally required for generating the DC, they are responsible for the nonlinear response of the system. Indeed, looking at Eqs. (22)–(26)

and comparing Fig. 5 with Fig. 6 one can see that the nonlinear dependence of the DC current on the transferred wave vector for any filling of the lowest miniband is a consequence of interband excitations (in the absence of the interband excitations i^{inter} and I_{AC} would be zero and the DC current I_{DC} would coincide with the current right after application of the HCP $I(t = 0^+)$).

5. Conclusions

We have calculated the probabilities of the transitions and the net charge current generated by half-cycle pulses in a superlattice under conditions in which the impulsive approximation is valid. The calculation is performed for times, which are much shorter than the relaxation time of carriers in a typical semiconductor superlattice (it is usually on the picosecond time scale). Application of appropriately designed half-cycle pulses results in indirect transitions and in a generation of a direct charge current, which is constant on a time scale smaller than the carriers relaxation time.

References

[1] R.F. Kazarinov, R.A. Suris, Sov. Phys. Semicond. 5 (1971) 707.
[2] C. Gmachl, F. Capasso, D.L. Sivco, A.Y. Cho, Rep. Prog. Phys. 64 (2001) 1533.
[3] L. Esaki, R. Tsu, IBM J. Res. Dev. 14 (1970) 61.
[4] E.L. Ivchenko, G.E. Pikus, Superlattices and Other Heterostructures, Springer, Berlin, 1997.
[5] P. Reimann, M. Grifoni, P. Hänggi, Phys. Rev. Lett. 79 (1997) 10.
[6] H. Linke, W. Sheng, A. Löfgren, H. Xu, P. Omling, P.E. Lindelof, Europhys. Lett. 44 (1998) 341.
[7] H. Linke, T.E. Humphrey, A. Löfgren, A.O. Sushkov, R. Newbury, R.P. Taylor, P. Omling, Science 286 (1999) 2314.
[8] I. Goychuk, P. Hänggi, Europhys. Lett. 43 (1998) 503.
[9] K.N. Alekseev, M.V. Erementchouk, F.V. Kusmartsev, Europhys. Lett. 47 (1999) 595.
[10] K.N. Alekseev, E.H. Cannon, J.C. McKinney, F.V. Kusmartsev, D.K. Campbell, Phys. Rev. Lett. 80 (1998) 2669.
[11] E.H. Cannon, F.V. Kusmartsev, K.N. Alekseev, D.K. Campbell, Phys. Rev. Lett. 85 (2000) 1302.
[12] D. You, R.R. Jones, P.H. Bucksbaum, D.R. Dykaar, Opt. Lett. 18 (1993) 290.
[13] R.R. Jones, D. You, P.H. Bucksbaum, Phys. Rev. Lett. 70 (1993) 1236.
[14] D. You, P.H. Bucksbaum, J. Opt. Soc. Am. B 14 (1997) 1651.
[15] A. Gürtler, C. Winnewisser, H. Helm, P.U. Jepsen, J. Opt. Soc. Am. A 17 (2000) 74.
[16] N.E. Tieckling, R.R. Jones, Phys. Rev. A 52 (1995) 1371.
[17] C.M. Dion, A. Keller, O. Atabek, Eur. Phys. J. D 14 (2001) 249.
[18] A. Matos-Abiague, J. Berakdar, Phys. Rev. A 68 (2003) 063411.
[19] A. Matos-Abiague, J. Berakdar, Europhys. Lett. 69 (2005) 277.
[20] A. Matos-Abiague, J. Berakdar, Phys. Rev. Lett. 94 (2005) 166801.
[21] E. Vanagas, Lithuanian Phys. J. 32 (1992) 330.
[22] E. Vanagas, Lithuanian Phys. J. 32 (1992) 371.
[23] E. Vanagas, Tech. Phys. Lett. 19 (1993) 408.
[24] S. Flügge, Practical Quantum Mechanics, Springer, Berlin, 1999.
[25] R. de L. Kronig, W.G. Penney, Proc. R. Soc. London A 130 (1931) 499.
[26] K. Vyborny, L. Smrcka, R.A. Deutschmann, Phys. Rev. B 66 (2002) 205318.
[27] N.E. Henriksen, Chem. Phys. Lett. 312 (1999) 196.
[28] D. Daems, S. Guerin, H.R. Jauslin, A. Keller, O. Atabek, Phys. Rev. A 69 (2004) 033411.
[29] E. Persson, S. Puschkarski, X.-M. Tong, Towards attosecond half-cycle pulses, in: F. Krausz (Ed.), International Conference on Ultrafast Optics, 2004, pp. 253–258.